

A First-Order Model for Computation of Laser-Induced Breakdown Thresholds in Ocular and Aqueous Media: Part II—Comparison to Experiment

Paul K. Kennedy, Stephen A. Boppart, Daniel X. Hammer, Benjamin A. Rockwell, Gary D. Noojin, and W. P. Roach

Abstract—An analytic, first-order model has been developed to calculate irradiance thresholds for laser-induced breakdown (LIB) in condensed media, including ocular and aqueous media. A complete derivation and description of the model was given in a previous paper (Part I). The model has been incorporated into a computer code and code results have been compared to experimentally measured irradiance thresholds for breakdown of ocular media, saline, and water by nanosecond, picosecond, and femtosecond laser pulses in the visible and near-infrared. The comparison included both breakdown data from the literature and from our own measurements. Theoretical values match experiment to within a factor of 2 or better, over a range of pulsewidths spanning five orders of magnitude.

I. INTRODUCTION

THE OPTICAL Radiation Division of Armstrong Laboratory is currently engaged in a multiyear experimental and theoretical research program to study how ultrashort laser pulses interact with, propagate through, and damage ocular tissue. One of the primary research goals is to gain an experimental and theoretical understanding of laser-induced breakdown (LIB) as a possible ocular damage mechanism. As a first step in understanding damage caused by LIB in the eye, experimental measurements and theoretical modeling are currently being performed to determine irradiance thresholds corresponding to breakdown in ocular media and in fluids used as simulants for ocular media, such as water and saline solution.

In a previous paper [1], a detailed derivation was given for an analytic, first-order model developed to calculate irradiance thresholds for laser-induced breakdown in condensed media, including ocular and aqueous media. The model was derived from the simple rate equation formalism of Shen [2] for cascade breakdown in solids and from the theory of multiphoton ionization in condensed media developed by Keldysh [3]. Analytic expressions were obtained for the irradiance thresholds corresponding to multiphoton breakdown, to cascade breakdown, and to initiation of cascade breakdown by multiphoton ionization of seed electrons (multiphoton initiation threshold).

Manuscript received March 24, 1995; revised July 28, 1995. This work was supported by Armstrong Laboratory and by the Air Force Office of Scientific Research (AFOSR) through Grant 2312AA-92AL014.

P. K. Kennedy, S. A. Boppart, D. X. Hammer, and B. A. Rockwell are with the Optical Radiation Division, Armstrong Laboratory, Brooks AFB, TX 78235 USA.

G. D. Noojin and W. P. Roach are with The Analytic Sciences Corporation, San Antonio, TX 78212 USA.

IEEE Log Number 9415338.

The model includes two different definitions of breakdown, corresponding to two different experimental endpoints. The “flash” endpoint (hot, dense, visibly emitting plasma) is calculated using critical densities of $10^{20}/\text{cm}^3$. The “bubble” endpoint (cooler, more diffuse plasma with little or no emission in the visible) is calculated using critical densities of $10^{18}/\text{cm}^3$. The model has been incorporated into a computer code for comparison to experiment.

This paper documents the code and gives a comparison of code results to experimentally measured irradiance thresholds for breakdown of ocular media, saline, and water by nanosecond (ns), picosecond (ps), and femtosecond (fs) laser pulses in the visible and near-infrared. The comparison includes data from the literature [4]–[8], for long pulse ($\tau_p \geq 30$ ps) infrared breakdown, and from our own measurements, for visible and infrared pulses ranging from 7 ns to 100 fs. Threshold values for visible wavelengths and for pulsewidths of less than 30 ps, have not, to our knowledge, previously been measured in these media.

Theoretical and experimental values agree fairly well for data corresponding to both experimental endpoints: 1. ns and long ps pulse breakdown with a flash endpoint, and 2. short ps and fs pulse breakdown with a bubble endpoint. Theoretical values match experiment to within a factor of 2 or better, over a range of pulsewidths spanning five orders of magnitude, a reasonably good match for a first order model.

A description of the code is given in Section II. Experimental equipment and techniques for the Armstrong Lab LIB measurements are described in Section III. In Sections IV and V experimental data is compared with code results for long pulse breakdown with a flash endpoint and for short pulse breakdown with a bubble endpoint, respectively. Conclusions are given in Section VI.

II. CODE DESCRIPTION

The Laser Induced Breakdown Irradiance Threshold code, or LIBIRT, incorporates the equations, parameters, and definitions of the model derived previously [1]. The code computes the cascade breakdown threshold, I_{th} , multiphoton breakdown threshold, I_{MP} , and multiphoton initiation threshold, I_m , for a specified medium, laser pulse, and breakdown end point. For pulsewidths too short to allow cascade breakdown from the minimum initial density, $\rho_o(\text{min})$, the code computes the alternate values I'_m and I'_{th} , corresponding to a higher initial

density $\rho'_o(\text{min})$. When the threshold for multiphoton initiation of a cascade is less than the threshold for sustaining the cascade to breakdown, the intermediate threshold $I''_m = I''_{\text{th}}$ is computed.

The code input parameters which characterize the laser pulse are the pulsewidth, τ_p , the wavelength, λ , and the beam diameter, d , at the breakdown region. (In agreement with the usual custom for Gaussian beams, d is defined as the diameter at the I_o/e^2 point.) Input parameters characterizing the medium are the ionization energy, E_{ion} , the index of refraction at the laser wavelength, n_o , the molecular mass, M , the momentum transfer collision time, τ , and the density of bound electrons with the specified ionization energy, ρ_b . Inputs which specify flash or bubble endpoint are the free electron critical density, ρ_{cr} and a logical flag whose value determines whether the code calculates thresholds for the bubble endpoint or the flash endpoint.

In addition to the parameters mentioned above, a number of other inputs are needed. The standard physical constants used in the model are hardwired into the code with at least 7 significant figures of accuracy. The minimum number of electrons which must be present in the focal volume to initiate cascade breakdown, $N_o(\text{min})$, is set to 1 for ns pulses and 10 for ps pulses. The number of collisions needed to absorb one photon, N_{coll} , was estimated to be 5 in all calculations.

Calculations are performed in FORTRAN double precision for greater accuracy. All values are computed in MKS units. For convenience irradiances are converted to W/cm^2 and electron densities to $1/\text{cm}^3$ prior to print-out.

III. ARMSTRONG LAB EXPERIMENTAL SET-UP

Researchers at Armstrong Lab have performed breakdown measurements on vitreous humor, saline, and water using infrared and visible laser pulses with pulsewidths ranging from 7 ns to 100 fs. In addition to the two papers describing the LIB model, a third paper, by Hammer *et al.* [9], has been written focusing on the experimental work. The experimental set-up used for breakdown measurements in liquid media, and the laser system which generates this wide range of short and ultrashort pulses, have been described in detail in [9], as well as in previous papers [10], [11]. Reference [9] also contains details of the statistical (probit) data analysis, such as slopes of probit curves and fiducial (95% confidence) limits on the ED_{50} probit values. Only a brief experimental description will be given here, as an introduction to the experimental data given in the next two sections.

A. Ultrashort Pulse Generation System

The Armstrong Lab laser pulse generation system can produce a wide variety of wavelengths, pulse durations, and energy levels. The system is modular and can be easily reconfigured for different pulsewidths. Only the shortest pulses require all units to operate simultaneously. Longer pulsewidths ($\tau_p \geq 50$ ps) can be produced at 10 Hz with maximum pulse energies of 40–50 millijoules (mJ). Shorter pulses ($\tau_p \leq 5$ ps) are also produced at 10 Hz with maximum pulse energies of 100–150 microjoules (μJ).

Long pulses are produced by two Spectra-Physics Nd:YAG lasers. A Q-switched DCR-11 produces pulses of 7–10 ns duration at 1064 nm. A GCR-3RA with frequency doubler produces Q-switched pulses of 3–7 ns at 532 nm and mode-locked pulses of 50–80 ps at 532 nm and 80 ps at 1064 nm.

Short pulses are produced by a six stage process, which begins with a Spectra-Physics 3800 Nd:YAG laser emitting a mode-locked train of 80 ps, 1064 nm pulses at a pulse repetition frequency (prf) of 82 megahertz (MHz). These pulses are compressed to 5 ps, frequency doubled, and used to pump a Spectra-Physics 3500 rhodamine dye laser. The output pulses from the dye laser, which may vary from 3 ps to 300 fs in duration, are chirped and spectrally broadened to 580 ± 10 nm, amplified in a three-stage pulse dye amplifier, and then spectrally rephased and temporally compressed. This process can produce 580 nm, 100 μJ pulses at 10 Hz with pulsewidths of 2–5 ps, 600–800 fs, 300–500 fs, or 80–120 fs, depending on the dye laser output and the degree of temporal compression.

B. Breakdown Measurements

For our ultrashort pulse breakdown experiments the liquid media were held in a quartz cell and the pulses focused into the cell using an aspheric lens with a focal length of 17 mm. This lens was chosen to approximate the 17.1 mm equivalent focal length of the human eye. The beam focal plane was 5–7 mm from the cell wall.

Visible plasmas produced by long pulse breakdown were detected with the naked eye, which is the standard detection method used for flash endpoint measurements. As noted previously [1], a problem arises in attempting to use the flash endpoint to detect breakdown by pulses shorter than 10 picoseconds. The intensity of the plasma radiation decreases as the pulsewidth becomes shorter and eventually becomes undetectable by the naked eye. Our short pulse measurements used a bubble endpoint, because no visible flashes were detected for our maximum available pulse energy ($\sim 100 \mu\text{J}$). To detect bubble formation following breakdown, the breakdown region of the cell was imaged with two lenses, of focal length 230 and 140 mm, onto a Hitachi CCTV camera. A 580 nm filter was added to the imaging system, in order to prevent reflected 580 nm laser light from complicating the bubble detection process.

For each medium and pulsewidth, 800 data points were taken covering a range of pulse energies. Statistical (probit) analysis was used to calculate the probability of breakdown as a function of pulse energy. The threshold, E_{BD} , was defined to be the energy corresponding to 50% probability of breakdown. The energy threshold, the pulsewidth, and the measured spot size at the focus, were then used to compute the irradiance threshold, I_{BD} .

The focal beam diameter at the I_o/e^2 point was determined by a knife edge measurement inside the water-filled cell. Spot sizes in the 20–30 μm range were measured for most pulsewidths, substantially greater than the theoretically calculated diffraction limit. Most of the deviation from the diffraction limit appears to arise from spherical aberrations produced by the air-media interface, although lens imperfec-

TABLE I
MATERIAL PARAMETERS OF WATER; USED IN THE CODE TO CALCULATE
THEORETICAL IRRADIANCE THRESHOLDS FOR WATER BREAKDOWN

E_{ion}	ionization energy	6.5 eV
$n_o(\lambda=1064 \text{ nm})$	index of refraction	1.32
$n_o(\lambda=580 \text{ nm})$	index of refraction	1.33
$n_o(\lambda=532 \text{ nm})$	index of refraction	1.34
M	molecular mass	$3.0 \times 10^{-26} \text{ kg}$
	momentum transfer collision time	$1.0 \times 10^{-15} \text{ sec}$
ρ_b	bound electron density	$6.68 \times 10^{23}/\text{cm}^3$

tions may also play some part. Further LIB measurements are planned with a system where the lens and the media are in direct contact. Hopefully this will reduce aberrations and produce a tighter focus. Spot sizes obtained with the current system, however, are close to the size of minimum visible lesions on the human retina ($\sim 20 \mu\text{m}$) and to the *in vivo* retinal spot size ($\sim 15\text{--}25 \mu\text{m}$) measured in primates [12], [13]. Experimental LIB thresholds obtained with these beams are also in fairly good agreement with theoretical values computed for the same spot size, as will be demonstrated in Sections IV and V.

Breakdown measurements were made using the vitreous humor of Dutch Belted Rabbits [14],¹ isotonic saline solution (0.9%), tap water, and two grades of high purity water, referred to as ultrapure and deionized. Deionized water was triply distilled to remove contaminants. Ultrapure water, obtained from Purity Water of San Antonio, TX, was triply distilled, UV irradiated to remove microbes, and degassed to parts per billion concentration of oxygen and nitrogen. It has a measured resistance of $18 \text{ M}\Omega/\text{cm}$.

All media used in our experiments can be categorized as either pure or impure water, including vitreous, which is essentially water with salts and collagen fibers added. Theoretical thresholds were therefore calculated for water breakdown, using the material parameters listed in Table I. For the exciton reduced mass in water, the estimate $m \approx m_h, m' \approx m/2$ was used. The model can simulate impure media, but only when the initial free electron density, ρ_o , is known for the medium in question and is specified as an input to the code. Since ρ_o was not known for any of the impure aqueous media used in this study, thresholds were calculated for water breakdown using the minimum initial density, $\rho_o(\text{min})$, as specified by the model [1]. As we will see in the next section, the impurity dependence of the experimental data for long pulse, cascade breakdown is fairly well explained by comparing the threshold for multiphoton initiation of cascade breakdown, I_m , with the threshold for sustaining a cascade to breakdown, I_{th} .

IV. LONG PULSE LIB WITH FLASH ENDPOINT

A number of researchers [4]–[8] have studied breakdown thresholds for ocular and aqueous media using both *Q*-switched (ns pulse) and mode-locked (ps pulse) Nd:YAG laser

¹The animals involved in this study were procured, maintained, and used in accordance with the Animal Welfare Act and [14].

emission at 1064 nm. This research was primarily motivated by the use of *Q*-switched Nd:YAG lasers in ophthalmic laser surgery [15], [16] and by the hope that mode-locked pulses might produce the same surgical effect at lower pulse energies and with less collateral tissue damage [7], [8].

Most of this long pulse breakdown work was done using the standard experimental endpoint of a hot, visibly emitting plasma; i.e., the flash endpoint. Some measurements on ps pulse breakdown, however, were made using detection of a cavitation bubble or a very weak flash as an endpoint [7], [8]. Data corresponding to a bubble endpoint will be discussed in Section V. In this section, we compare the code results for long pulse breakdown with a flash endpoint both to the experimental data in the literature and to our own measurements.

As mentioned in Section III, we measured the actual spot sizes produced by our experimental set-up at all pulsewidths where data was taken. As the actual beam sizes are known, the average irradiance threshold over the breakdown spot, I_{BD} , can be calculated with reasonable accuracy, providing a valid comparison with theoretical irradiance thresholds computed from the model. Unfortunately, the data available in the literature [4]–[8] gives only (calculated) diffraction-limited beam waists. Comparison of experimental irradiance thresholds computed using diffraction-limited spot sizes to theoretical values from the model must be approached with caution. Discrepancies can be expected whenever the actual beam size deviates significantly from the diffraction limit.

A. Docchio and Sacchi

The most useful data in the literature, for comparison to the model, are the results of Docchio *et al.* [5], [6] and Sacchi [4]. These LIB measurements were made using large diameter beams and the actual spot sizes were apparently close to diffraction-limited values. At any rate, experimental irradiances computed using these diffraction-limited spot sizes agreed well with theoretical values computed for the same beam diameters.

Unfortunately, the irradiances reported in [4]–[6] are calculated using the beam diameter at the I_o/e point, rather than the I_o/e^2 diameter assumed in the model as the standard for gaussian beams. In order to scale the experimental data for comparison to the code results, we use the relationship between the two diameters of an ideal Gaussian beam

$$d[I_o/e^2] = 2^{1/2} d[I_o/e]. \quad (1)$$

Use of the measured single pulse energy threshold, E_{BD} , with the larger beam diameter, $d[I_o/e^2]$, gives an average irradiance $1/2$ the listed value in [4]–[6], since the beam area is a factor of two larger.

Table II lists the (scaled) experimental irradiance thresholds for breakdown of calf vitreous, saline, tap water, and distilled water by 7 ns, Nd:YAG laser pulses. Data was taken for (I_o/e) beam diameters from 50–350 μm , giving (I_o/e^2) beam diameters from 70.7–495 μm , when (1) is used. Thresholds representing both 50 and 100% probability of breakdown (flash

TABLE II
EXPERIMENTAL AND THEORETICAL IRRADIANCE THRESHOLDS FOR BREAKDOWN [FLASH ENDPOINT] OF WATER, SALINE, AND VITREOUS BY 7 ns, Nd:YAG LASER PULSES. EXPERIMENTAL DATA IS FROM [4]–[6]

Ref., τ_p , λ	$d(\mu\text{m})^3$	Medium	$I_{BD}(\text{W}/\text{cm}^2)$ 100% ⁵	$I_{BD}(\text{W}/\text{cm}^2)$ 50% ⁵	$I_{BD}(\text{W}/\text{cm}^2)$ Code ⁶
Docchio ¹ $\tau_p = 7$ nsec $\lambda = 1064$ nm	70.71	Distilled-H ₂ O	2.1×10^{10}	1.5×10^{10}	$I_m = 1.78 \times 10^{10}$ $I_a = 1.77 \times 10^9$
		Saline	1.85×10^{10}	1.25×10^{10}	
		Vitreous ⁴	1.5×10^{10}	1.02×10^{10}	
		Tap-H ₂ O	3.0×10^9	2.0×10^9	
Sacchi ² $\tau_p = 7$ nsec $\lambda = 1064$ nm	106.1	Distilled-H ₂ O	1.73×10^{10}	-----	$I_m = 1.36 \times 10^{10}$ $I_a = 1.79 \times 10^9$
Docchio ¹ $\tau_p = 7$ nsec $\lambda = 1064$ nm	132.9	Distilled-H ₂ O	1.55×10^{10}	-	$I_m = 1.17 \times 10^{10}$ $I_a = 1.80 \times 10^9$
		Saline	1.35×10^{10}	----	
		Vitreous ⁴	1.17×10^{10}	-	
		Tap-H ₂ O	2.6×10^9	----	
Docchio ¹ $\tau_p = 7$ nsec $\lambda = 1064$ nm	325.3	Distilled-H ₂ O	6.85×10^9	---	$I_m = 6.43 \times 10^9$ $I_a = 1.86 \times 10^9$
		Saline	6.5×10^9	--	
		Vitreous ⁴	4.55×10^9	-	
		Tap-H ₂ O	1.7×10^9	-----	
Docchio ¹ $\tau_p = 7$ nsec $\lambda = 1064$ nm	495.0	Distilled-H ₂ O	5.3×10^9	2.5×10^9	$I_m = 4.86 \times 10^9$ $I_a = 1.89 \times 10^9$
		Saline	4.25×10^9	2.25×10^9	
		Vitreous ⁴	3.5×10^9	2.0×10^9	
		Tap-H ₂ O	1.5×10^9	0.9×10^9	

1. F. Docchio, *et al.*, Refs. 5 and 6.

2. C. A. Sacchi, Ref. 4.

3. Calculated beam diameter at I_0/e^2 point ($\approx 2^{1/2}$ times d at I_0/e point).

4. Calf vitreous.

5. Experimental thresholds for 100% or 50% probability of breakdown [flash endpoint]. Irradiances listed are 1/2 the values in Refs. 4–6, due to use of d at the I_0/e^2 point.

6. Theoretical thresholds for flash endpoint.

endpoint) are reported. The data shows a strong impurity dependence, with the purest medium, distilled water, having a threshold 4–7 times higher than that of tap water. The dominant mechanism for breakdown in this pulsewidth and wavelength regime is clearly impurity dependent cascade ionization. For pure water, in the absence of impurities which provide seed electrons, breakdown should occur through cascade ionization with multiphoton initiation.

The theoretical thresholds for cascade and multiphoton breakdown in water were calculated for the flash endpoint using the laser parameters of Table II. Irradiances needed for “pure” multiphoton breakdown are two to three orders of magnitude higher than experimentally measured values. On the other hand, the thresholds for cascade breakdown and multiphoton initiation, I_{th} and I_m , are in good agreement with the data and are listed in Table II.

In this pulsewidth and wavelength regime, $I_m > I_{th}$. For pure water, where both multiphoton initiation and cascade breakdown conditions must be satisfied, the measured value should correspond to the higher threshold, I_m . For aqueous media impure enough to provide their own seed electrons, multiphoton initiation is not needed and I_{th} should be the measured value. As can be seen from Table II, the measured values for distilled water and tap water are roughly equivalent to I_m and I_{th} , respectively, consistent with the theoretical analysis above. In Fig. 1, the values for distilled water breakdown are plotted along with I_m . In every case the theoretical value lies

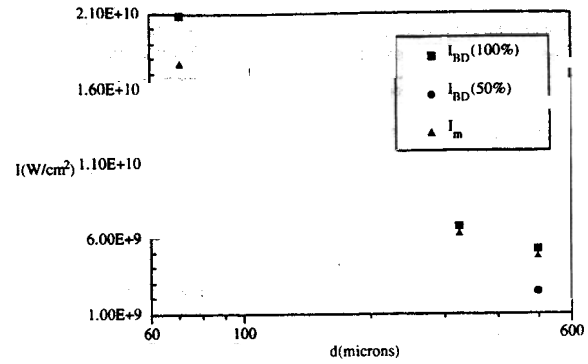


Fig. 1. Irradiance threshold versus spot size for distilled water breakdown by 7-ns, 1064-nm pulses. Experimental data is from [4]–[6].

TABLE III
EXPERIMENTAL AND THEORETICAL THRESHOLDS FOR LONG PULSE BREAKDOWN [FLASH ENDPOINT] OF WATER, SALINE, AND VITREOUS. ALL EXPERIMENTAL DATA BY S. BOPPART

Ref., τ_p , λ	$d(\mu\text{m})^1$	Medium	$E_{BD}(\mu\text{J})$ Exper. ³	$I_{BD}(\text{W}/\text{cm}^2)$ Exper. ³	$I_{BD}(\text{W}/\text{cm}^2)$ Code ⁴
S. Boppart $\tau_p = 7$ nsec $\lambda = 1064$ nm	22.0	Ultrapure-H ₂ O	483	1.82×10^{10}	$I_m = 3.87 \times 10^{10}$ $I_a = 1.70 \times 10^9$
		Vitreous ²	338	1.27×10^{10}	
		Saline	221	8.31×10^9	
		Tap-H ₂ O	150	5.64×10^9	
S. Boppart $\tau_p = 3$ nsec $\lambda = 532$ nm	26.0	Ultrapure-H ₂ O	140	8.79×10^9	$I_m = 7.06 \times 10^9$
		Saline	159	9.98×10^9	
		Tap-H ₂ O	149	9.35×10^9	
S. Boppart $\tau_p = 80$ psec $\lambda = 1064$ nm	26.0	Ultrapure-H ₂ O	80.7	1.90×10^{11}	$I_m = 1.07 \times 10^{11}$
		Saline	82.0	1.93×10^{11}	
		Tap-H ₂ O	81.1	1.91×10^{11}	

1. Measured beam diameter at I_0/e^2 point.

2. Dutch Belted Rabbit vitreous.

3. Experimental thresholds for 50% probability of breakdown [flash endpoint].

4. Theoretical thresholds for flash endpoint.

below the measured value for 100% probability of breakdown and above the 50% value.

B. Armstrong Lab Data

Researchers at Armstrong Lab have measured LIB thresholds for long pulses at both visible and infrared wavelengths. Table III shows the experimentally measured energy and irradiance thresholds for breakdown of rabbit vitreous, saline, ultrapure water, and tap water, using 7-ns pulses at 1064 nm, 3-ns pulses at 532 nm, and 80-ps pulses at 1064 nm. This data was taken by S. Boppart and represents the flash endpoint.

As with the Docchio and Sacchi data, calculated multiphoton breakdown thresholds were found to be several orders of magnitude higher than experimental values, indicating cascade ionization as the dominant mechanism in all cases. The theoretical thresholds for cascade breakdown are listed in Table III, next to the corresponding experimental values. The match between theory and experiment in the 7-ns data of Table III is not as good as the match with the Docchio and Sacchi data at the same pulsewidth and wavelength. Nevertheless, the theoretical and experimental values agree to within a factor of 2 for all three pulsewidths.

Note that the strong impurity dependence seen for the 7-ns data largely disappears for the shorter pulsewidths, despite the fact that cascade ionization is still dominant. The same trend can be seen in the data of Docchio *et al.* [6] for aqueous and vitreous breakdown by 1064 nm pulses of various durations. The impurity dependence seen for the 7 ns data is greatly reduced at 220 ps and essentially vanishes at 30 ps. Use of the code to study trends in the threshold values as a function of pulsewidth offers an explanation. For long pulses, $I_m > I_{th}$. For fixed wavelength and spot size, both thresholds will increase as the pulsewidth decreases, but the cascade breakdown threshold rises faster and will eventually become larger.

As explained previously [1], when a regime is reached where $I_{th}[\rho_o = \rho_o(\min)] > I_m$, then the measured threshold will be the intermediate value $I_m'' = I_{th}''$. Here, I_m'' represents the new multiphoton initiation threshold, which generates an initial density $\rho_o'' > \rho_o(\min)$, and the equivalent value I_{th}'' represents the irradiance needed to sustain a cascade from ρ_o'' to breakdown. In such circumstances, or even when $I_m \approx I_{th}$, the impurity dependence of the cascade breakdown process essentially vanishes. Any field at the threshold level will simultaneously generate its own seed electrons *and* provide the irradiance needed to sustain the cascade to breakdown. The initial free electron density in the medium thus becomes unimportant, unless it is unusually high ($\rho_o > \rho_o''$).

C. Zysset and Vogel

Zysset *et al.* [7] and Vogel *et al.* [8] have made detailed studies of aqueous breakdown by Nd:YAG laser emission and have measured not only breakdown thresholds; but also plasma volume, cavitation bubble size and duration, and shock wave velocity, corresponding to suprathreshold breakdown. As in [4]–[6], threshold irradiances are computed using the (calculated) diffraction-limited beam waist rather than the actual measured spot size.

Table IV shows experimental data from [7] and [8] for breakdown of water and saline by Q-switched, ns duration, Nd:YAG laser pulses. Corresponding Armstrong Lab data is also listed for comparison. Single pulse energy thresholds are similar for all three studies, as are the diffraction-limited spot sizes ($\sim 4 \mu\text{m}$).

The irradiances listed in Table IV are significantly higher than the theoretical values predicted by the model for these diffraction-limited spot sizes. It is reasonable to assume that the tight focusing geometries caused greater deviation from the diffraction limit than occurred in the large beam data of [4]–[6]. The actual beam diameter for the 7 ns Armstrong Lab data was measured to be $22 \mu\text{m}$, as seen in Table III.

Using the code, a parameter study was performed to try and estimate the probable spot size for the data of [7] and [8]. The experimental energy thresholds were used with larger (estimated) beam diameters, to calculate lower (estimated) experimental irradiances, which were then compared to code results for the same estimated spot sizes. Beam diameters of $8 \mu\text{m}$ were found to produce an approximate match between theoretical and experimental values for the Zysset and Vogel

TABLE IV
EXPERIMENTAL THRESHOLDS FOR LONG PULSE BREAKDOWN [FLASH ENDPOINT] OF WATER AND SALINE. IRRADIANCE THRESHOLDS ARE CALCULATED USING THE DIFFRACTION-LIMITED SPOT SIZE

Ref.	τ_p, λ	$d(\mu\text{m})^3$	Medium	$I_{th}(\text{W/cm}^2)$ Exper. ⁴	$E_{th}(\mu\text{J})$ Exper. ⁴
Zysset, et al. ¹	10 nsec	4	Deion.-H ₂ O	3.2×10^{11}	400
	1064 nm		Saline	3.0×10^{11}	380
			Tap-H ₂ O	1.8×10^{11}	226
Vogel, et al. ²	6 nsec 1064 nm	3.7	Distilled-H ₂ O	3.1×10^{11}	200
S. Boppart	7 nsec	3.6	Ultrapure-H ₂ O	6.78×10^{11}	483
	1064 nm		Saline	3.10×10^{11}	221
			Tap-H ₂ O	2.10×10^{11}	150

1. B. Zysset, et al., Ref. 7.

2. A. Vogel, et al., Ref. 8.

3. Calculated (diffraction-limited) beam diameter at L/e^2 point.

4. Experimental thresholds for 50% probability of breakdown [flash endpoint].

data. A more exact comparison between the theory and this data is impossible without measurements of the true spot size.

V. SHORT PULSE LIB WITH BUBBLE ENDPOINT

In addition to the ns pulse measurements just discussed, the studies of Zysset and Vogel included measurements of mode-locked, ps pulse, Nd:YAG breakdown and its aftereffects. The experimental endpoints used, however, were somewhat different for ps breakdown. Zysset used detection of a cavitation bubble, produced as an aftereffect of plasma formation, as an endpoint. Vogel used a flash endpoint; but it was not the bright, easily visible flash seen in ns pulse breakdown. Rather it was an extremely weak flash, barely visible in a darkened room, to a researcher with dark-adapted vision [17]. This seems much closer to bubble endpoint criteria than to the standard flash endpoint. The threshold energy measured for this endpoint also corresponds more closely to the low-pulse energies required for bubble formation than to the high pulse energies needed for a bright, easily visible flash.

In this section, we compare the code results for short pulse breakdown with a bubble endpoint to the Zysset and Vogel ps data and to our own measurements of ps and fs pulse breakdown.

A. Armstrong Lab Data

A bubble endpoint, similar to that of Zysset, has been used in our measurements of LIB thresholds for ultrashort ($\tau_p \leq 5$ ps) pulses at 580 nm. We did not attempt to detect the expansion and collapse of the initial cavitation bubble, which occurs on microsecond time scales [18]. Instead we looked for the smaller and longer lasting bubbles produced in the focal region by diffusion of gas into the oscillating cavitation bubble [19]. Bubble formation was observed at threshold energies of only a few microjoules per pulse. On the other hand, pulse energies two orders of magnitude higher (100–150 μJ), which represent the highest energies available with our current system, were insufficient to produce flashes visible to the naked eye.

TABLE V
EXPERIMENTAL AND THEORETICAL THRESHOLDS FOR
SHORT PULSE BREAKDOWN [BUBBLE ENDPOINT] OF WATER
AND SALINE. ALL EXPERIMENTAL DATA BY D. HAMMER

Ref., τ_p , λ	$d(\mu\text{m})^1$	Medium	$E_{\text{BD}}(\mu\text{J})$ Exper. ²	$I_{\text{BD}}(\text{W}/\text{cm}^2)$ Exper. ²	$I_{\text{BD}}(\text{W}/\text{cm}^2)$ Code ³
D. Hammer $\tau_p = 2.4$ psec $\lambda = 580$ nm	21.0	Deionized-H ₂ O	4.08	4.91×10^{11}	$I_m'' = 6.66 \times 10^{11}$
		Saline	4.17	5.02×10^{11}	
		Tap-H ₂ O	4.15	4.99×10^{11}	
D. Hammer $\tau_p = 400$ fsec $\lambda = 580$ nm	22.0	Deionized-H ₂ O	1.92	1.26×10^{12}	$I_m'' = 2.56 \times 10^{12}$
		Saline	1.99	1.31×10^{12}	
		Tap-H ₂ O	1.92	1.26×10^{12}	
D. Hammer $\tau_p = 100$ fsec $\lambda = 580$ nm	17.0	Deionized-H ₂ O	1.31	5.77×10^{12}	$I_{\text{MP}} = 5.46 \times 10^{12}$
		Saline	1.27	5.60×10^{12}	
		Tap-H ₂ O	1.27	5.60×10^{12}	

1. Measured beam diameter at L/e^2 point.

2. Experimental thresholds for 50% probability of breakdown [bubble endpoint].

3. Theoretical thresholds for bubble endpoint.

Table V shows the experimentally measured energy and irradiance thresholds for breakdown of saline, deionized water, and tap water, using 2.4 ps, 400 fs, and 100 fs pulses at 580 nm. This data was taken by D. Hammer. Code values, listed for comparison, are once again within a factor of two of measured thresholds.

None of the threshold data for short pulse breakdown shows any significant impurity dependence, a fact which has different theoretical explanations in different pulsewidth regimes. Both the 2.4 ps and 400 fs data represent cascade breakdown regimes, where the threshold defined by the model is the intermediate value $I_m'' = I_{\text{th}}''$. As explained in Section IV-B, little or no impurity dependence should be present in such regimes. At 100 fs, the model predicts that the measured threshold should correspond to the value for "pure" multiphoton breakdown, I_{MP} , and multiphoton breakdown is not an impurity dependent process.

As described in the previous paper [1], the model has special provisions for calculating cascade breakdown thresholds for extremely short pulses. In the subpicosecond regime, it may not be possible to achieve cascade multiplication from the minimum initial density, $\rho_o(\text{min})$, to the critical density, ρ_{cr} , during the time that the field is present. In this case a higher minimum initial density, $\rho_o'(\text{min})$, is defined, for which breakdown can be achieved in the time available, and new thresholds I_m' and I_{th}' , corresponding to the new initial density, are calculated.

Code results show that such calculations were needed for both the 400 and 100 fs pulses, with the required initial densities being approximately $10^{12}/\text{cm}^3$ and $10^{16}/\text{cm}^3$, respectively. The latter is almost equivalent to the $10^{18}/\text{cm}^3$ critical density used for the bubble endpoint. Cascade breakdown clearly cannot take place in these pulsewidth regimes without a significant "jump start" from multiphoton ionization. Even with multiphoton ionization providing high initial densities, the computed cascade breakdown threshold at 100 fs was higher than the threshold for pure multiphoton breakdown. The multiphoton breakdown threshold is therefore the value reported in Table V and is in good agreement with the measured value.

TABLE VI
EXPERIMENTAL THRESHOLDS FOR SHORT PULSE BREAKDOWN (BUBBLE
OR WEAK FLASH ENDPOINT) OF WATER AND SALINE. IRRADIANCE
THRESHOLDS ARE CALCULATED USING THE DIFFRACTION-LIMITED SPOT SIZE

Ref. [endpoint]	τ_p , λ	$d(\mu\text{m})^3$	Medium	$I_{\text{BD}}(\text{W}/\text{cm}^2)$ Exper. ⁴	$E_{\text{BD}}(\mu\text{J})$ Exper. ⁴
Zysset, et al. ¹ [bubble]	40 psec 1064 nm		Deion.-H ₂ O	1.6×10^{12}	
			Saline	1.0×10^{12}	5
			Tap-H ₂ O	0.5×10^{12}	2.5
Vogel, et al. ² [weak flash]	30 psec 1064 nm	4.3	Distilled-H ₂ O	3.4×10^{12}	15
D. Hammer [bubble]	2.4 psec 580 nm	1.8	Deion.-H ₂ O	6.68×10^{13}	4.08
			Saline	6.83×10^{13}	4.17
			Tap-H ₂ O	6.80×10^{13}	4.15

1. B. Zysset, et al., Ref. 7.

2. A. Vogel, et al., Ref. 8.

3. Calculated (diffraction-limited) beam diameter at L/e^2 point.

4. Experimental thresholds for 50% probability of breakdown [bubble or weak flash endpoint].

From the experimental data and from results of theoretical calculations, we can identify three regimes for aqueous breakdown. 1) For $\tau_p \geq 1$ ps, breakdown is by cascade ionization (with multiphoton initiation required for pure media). 2) For subpicosecond pulses down to ~ 200 fs, breakdown begins with multiphoton ionization providing high initial densities and then is completed by cascade ionization. This is the multiphoton "jump start" regime mentioned above. 3) Below 200 fs a transition occurs from multiphoton-assisted cascade breakdown to pure multiphoton breakdown, with the exact transition point depending on the laser wavelength. At 580 nm code runs indicate a transition around 160–170 fs. It is interesting to compare this with the results of Du *et al.*, [20] for LIB in fused silica produced by ultrashort pulses from a Ti:sapphire-based laser system. They concluded that breakdown was by multiphoton-assisted cascade down to 150 fs.

B. Zysset and Vogel

Table VI shows the Zysset and Vogel threshold data for ps pulse, Nd:YAG breakdown of water and saline. The D. Hammer data for breakdown by 2.4 ps, 580 nm pulses is also shown for comparison. Although both the wavelengths and the pulsewidths are significantly different, the threshold energies measured by Zysset and Hammer for bubble formation are of the same order of magnitude.

Once again, only values corresponding to diffraction-limited spots are reported in [7] and [8], and these irradiances are much higher than values predicted by the model. As before a parameter study was performed with the code to estimate the probable spot size. In this case, beam diameters of $12 \mu\text{m}$ were found to produce an approximate match between theoretical and experimental values.

VI. CONCLUSION

The results of an analytic, first-order model for computation of LIB thresholds in condensed media, have been compared to a wide range of experimental data for breakdown of ocular and aqueous media by ns, ps, and fs pulses in the visible

and near-infrared. Theoretical and experimental values agree fairly well for data corresponding to two different experimental endpoints: 1) ns and long ps pulse breakdown with a flash endpoint, and 2) short ps and fs pulse breakdown with a bubble endpoint. Theoretical values match experiment to within a factor of 2 or better, over a range of pulsewidths spanning five orders of magnitude, a reasonably good match for a first order model.

The code has proven useful in explaining trends in the threshold data, such as the presence or absence of impurity dependence, the link between measured cascade breakdown thresholds and multiphoton initiation requirements, and the transition from cascade to multiphoton ionization as the dominant breakdown mechanism at ultrashort pulsewidths. It may also be useful in the future as part of a larger end-to-end model of optical propagation and damage in the eye.

ACKNOWLEDGMENT

The authors would like to thank Dr. A. Vogel for valuable discussions on short pulse LIB in aqueous media.

REFERENCES

- [1] P. K. Kennedy, "A first-order model for computation of laser-induced breakdown thresholds in ocular and aqueous media: Part I—Theory," *IEEE J. Quantum Electron.*, this issue, pp. 2241–2249.
- [2] Y. R. Shen, *The Principles of Nonlinear Optics*. New York: Wiley, 1984, pp. 528–539.
- [3] L. V. Keldysh, "Ionization in the field of a strong electromagnetic wave," *Sov. Phys. JETP*, vol. 20, pp. 1307–1314, 1965.
- [4] C. A. Sacchi, "Laser-induced electric breakdown in water," *J. Opt. Soc. Am. B*, vol. 8, pp. 337–345, 1991.
- [5] F. Docchio, L. Dossi, and C. A. Sacchi, "Q-switched Nd:YAG laser irradiation of the eye and related phenomena: An experimental study. I. Optical breakdown determination for liquids and membranes," *Lasers in the Life Sci.*, vol. 1, pp. 87–103, 1986.
- [6] F. Docchio, C. A. Sacchi, and J. Marshall, "Experimental investigation of optical breakdown thresholds in ocular media under single pulse irradiation with different pulse durations," *Lasers in Ophthalmol.*, vol. 1, pp. 83–93, 1986.
- [7] B. Zysset, J. G. Fujimoto, and T. F. Deutsch, "Time-resolved measurements of picosecond optical breakdown," *Appl. Phys. B*, vol. 48, pp. 139–147, 1989.
- [8] A. Vogel, S. Busch, K. Jungnickel, and R. Birngruber, "Mechanisms of intraocular photodisruption with picosecond and nanosecond laser pulses," *Lasers in Surgery and Med.*, vol. 15, pp. 32–43, 1994.
- [9] D. X. Hammer, R. J. Thomas, G. D. Noojin, B. A. Rockwell, P. K. Kennedy, and W. P. Roach, "Experimental investigation of ultrashort pulse laser-induced breakdown thresholds in aqueous media," submitted to *IEEE J. Quantum Electron.*, 1995.
- [10] D. X. Hammer, R. Eiserer, G. D. Noojin, S. A. Boppart, P. K. Kennedy, and W. P. Roach, "Temperature dependence of laser-induced breakdown," in *Laser-Tissue Interaction V*, S. L. Jacques, Ed., *Proc. SPIE*, vol. 2134A, pp. 38–48, 1994.
- [11] S. A. Boppart, C. A. Toth, W. P. Roach, and B. A. Rockwell, "Shielding effectiveness of femtosecond laser-induced plasmas in ultrapure water," in *Laser-Tissue Interaction IV*, S. L. Jacques, Ed., *Proc. SPIE*, vol. 1882, pp. 347–354, 1993.
- [12] L. D. Forster, "Light intensity measurements with a fiber optic microprobe in the laser irradiated rhesus monkey eye," dissertation, Univ. of Texas at Austin, 1978.
- [13] G. D. Polhamus, D. K. Cohoon, and R. G. Allen, "Measurement of the point spread function in the rhesus eye," Tech. Pap., USAF School of Aerospace Med., 1979.
- [14] *Guide for the Care and Use of Laboratory Animals*. Washington, DC: Inst. of Lab. Animal Resources—Nat. Res. Council.
- [15] S. J. Gitomer and R. D. Jones, "Laser-produced plasmas in medicine," *IEEE Trans. Plasma Sci.*, vol. 19, pp. 1209–1219, 1991.
- [16] M. J. C. van Gemert and A. J. Welch, "Clinical use of laser-tissue interactions," *IEEE Eng. Med. and Biol.*, pp. 10–13, Dec. 1989.
- [17] A. Vogel, personal communication.
- [18] A. Vogel and W. Lauterborn, "Acoustic transient generation by laser-produced cavitation bubbles near solid boundaries," *J. Acoust. Soc. Am.*, vol. 84, pp. 719–731, 1988.
- [19] C. C. Church, "A theoretical study of cavitation generated by an extracorporeal shock wave lithotripter," *J. Acoust. Soc. Am.*, vol. 86, pp. 215–227, 1989.
- [20] D. Du, X. Liu, G. Korn, J. Squier, and G. Mourou, "Laser-induced breakdown by impact ionization in SiO₂ with pulse widths from 7 ns to 150 fs," *Appl. Phys. Lett.*, vol. 64, pp. 3071–3073, 1994.

Paul K. Kennedy, for a photograph and biography, see this issue, p. 2249.



Stephen A. Boppart was born in Harvard, IL, in 1968. He received the B.S. and M.S. degrees in electrical engineering with a bioengineering option from the University of Illinois at Urbana-Champaign in 1990 and 1991, respectively.

Since 1991, he has been with the Air Force's Armstrong Laboratory conducting research in the area of laser-tissue interactions in ocular structures. Currently, he is pursuing the Ph.D. degree at the Massachusetts Institute of Technology and the M.D. degree at Harvard University. His research interests

include laser applications in medicine and medical imaging.

Mr. Boppart is a member of OSA, APS, SPIE, Eta Kappa Nu, and Tau Beta Pi.



Daniel X. Hammer received the B.S. degree in electrical engineering from Rensselaer Polytechnic Institute, Troy, NY, in 1991.

He was commissioned in the Air Force in 1992 and is currently a research engineer in the Optical Radiation Division of Armstrong Laboratory at Brooks Air Force Base, Texas. His research interests include biomedical optics, laser-induced breakdown, and other biomedical effects of ultrashort laser pulses.

Mr. Hammer is a member of SPIE and OSA.



Benjamin A. Rockwell received the B.S. degree in physics in 1986 from Central Missouri State University and the Ph.D. degree in physics in 1991 from the University of Missouri-Columbia.

He is a Research Biophysicist at the Air Force Armstrong Laboratory, Optical Radiation Division, Optical Biophysics Branch, Brooks Air Force Base, TX, working in the field of laser-tissue interactions. He is currently the technical manager for an Air Force Office of Scientific Research-sponsored research effort entitled "Ultrashort Laser Pulse Effects

in Biological and Related Media." He is presently studying the nonlinear optical properties of ocular media as part of an effort to understand retinal damage produced by ultrashort laser pulses.

Dr. Rockwell is a member of SPIE, BiOS, APS, and OSA.



Gary D. Noojin received the A.A.S. degree in electronic engineering technology in 1986 from the National Education Center and is pursuing a computer science degree from Texas Lutheran College.

He is an electro-optics technician for TASC, Inc. He has 13 years experience in electronics and related fields. Since 1990, he has operated and maintained the ultrashort pulse laser systems at the Air Force Armstrong Laboratory, Optical Radiation Division. He is currently the chief technician for a group of researchers studying the effects of laser-induced

breakdown and other ultrashort pulse damage mechanisms.



William P. Roach received the B.A. degree in chemistry and mathematics from Avial College in 1983, and the M.S. and Ph.D. degrees in physics from the University of Missouri-Columbia in 1986 and 1990, respectively.

He is currently the Chief of the Optical Biophysics Branch, Optical Radiation Division, at the Air Force's Armstrong Laboratory, Brooks AFB, TX. He is the consultant to the Air Force Surgeon General for laser application and use, and directs research for the United States Air Force designed

to address issues involving ocular laser safety for National and Air Force interests.

Dr. Roach is a member of Sigma Pi Sigma, APS, OSA, and SPIE.